

MR T1 Image Segmentation of a Prostate Based on Distance Regularized Level Set Evolution

Yong-de Zhang¹, Jing-chun Peng^{1,2}, Gang Liu¹, Jin-gang Jiang¹ and Yan-jiang Zhao¹

¹*Intelligent Machine Institute, Harbin University of Science and Technology, China*

²*Harbin Huade University, China*
zhangyd@hrbust.edu.cn, pjc8996@126.com

Abstract

Prostate segmentation from MRI is a necessary first step and plays an important role in clinical decision making process. A MR T1 Image segmentation method of the prostate based on distance regularized level set evolution (DRLSE) is proposed. To smooth the prostate image to reduce the noise, a preprocessed prostate image with Gaussian kernel and get an edge indicator is convolved. We construct an energy function with a distance regularization term and an external energy term containing the edge indicator and minimize it by solving the gradient flow which can be implemented with a finite difference scheme. In segmentation experiments, the impact of parameters λ , μ , α and ε in DRLSE model on the image segmentation is analyzed, and an optimal value of these parameters is given. The experiment results confirm the effectiveness of the MRI segmentation method of prostate for different situation of different patients.

Keywords: *Image segmentation, Prostate, Magnetic resonance imaging, Level set, Active contours model*

1. Introduction

Prostate cancer is the most common malignant tumor in male. The clinic treatment shows that if prostate cancer is detected early, men have a higher survival rate. Therefore, there is a high value on prostate cancer diagnosis and treatment. Magnetic resonance imaging (MRI) has higher accuracy in the detection of prostate cancer and is considered to be the most effective imaging techniques at present[1]. Prostate segmentation from MRI is a necessary first step and plays a key role in different stages of clinical decision making process [2-7]. However, manual segmentation of a prostate is a laborious and time consuming work and different physician is easy to make the different segmentation results. So, accurate computerized prostate segmentation based on MRI is extremely useful. But, this task is very challenging because of the noise and inhomogeneity of MRI and the complex anatomical structures of prostate and surrounding organs.

In literatures, a variety of methods have been presented for prostate segmentation based on MRI. Shekhar Chandra [8] utilized a deformable model by initialization and training to accurately segment the prostate. S. Ghose[9] used graph cut by energy minimization in a stochastic domain obtained with atlas to realize the segmentation of prostate in MRI. Shekhar Chandra [10] built case specific atlases from training images and used a multi-atlas non-rigid registration method to realize more accurate location of the prostate. Yusuf Artan[11] developed a Multispectral Random Walks method using gradient based optimization algorithm to yield improved segmentation performance of the prostate. The Active Shape Model is a popular segmentation method. M. Yang and X. Li[12] proposed a distinctive image appearance descriptor that was incorporated in the active shape model

to segment the prostate from T2W MRI. Xin Liu[13] utilized region-based active contour model and shape information to segment prostate without training dataset. Wei Xiong[14] realized the accurate prostate segmentation by combining 3D graph cuts and 3D geodesic active contour shape prior level set. R. Toth and A. Madabhushi[15] presented a novel active appearance models methodology that utilized the level set to realize the most accurate segmentation. Level set as a more effective method of the prostate segmentation based on MRI has a certain advantage. However, the level set function (LSF) typically develops irregularities during its evolution, which cause numerical errors and eventually destroy the stability of the level set evolution. To overcome these problems, the reinitialization is performed by periodically stopping the evolution and reshaping the degraded LSF as a signed distance function. However, when and how the reinitialization should be performed introduces more serious problems and affects the accuracy in an undesirable way. Chunming Li[16]proposed an idea of distance regularized level set evolution that needn't reinitialization and avoided the numerical errors.

The paper is organized as follows. After introduction, the DRLSE method presented in [16] is described in section 2. Then, a MR T1 image segmentation method of a prostate based on DRLSE method is presented in section 3. Next, in section 4, the experimental results are discussed. The paper ends typically with conclusions and references.

2. DRLSE

LSF proposed by Chunming Li[16] could maintain the regularity during evolution. The level set evolution was implemented by minimizing an energy function with a distance regularization term and an external energy term. The energy function minimized would drive the motion of the contour toward desired locations .The level set evolution induced a surrounding diffusion effect that could maintain the desired shape and the distance near the desired contour. This level set evolution proposed is called distance regularized level set evolution (DRLSE).

An interested contour is embedded as the zero level set of an LSF. The LSF should be smooth and not too steep or too flat during the evolution. This condition is well satisfied by signed distance function, $|\nabla\phi|=1$ which is referred to as the signed distance property. In this section, LSF that has an intrinsic mechanism of maintaining this desirable property is described.

Firstly, Let $\phi:\Omega\rightarrow\Re$ be a LSF defined on a domain Ω , an energy function $\varepsilon(\phi)$ is defined by

$$\varepsilon(\phi) = \mu R_p(\phi) + \varepsilon_{\text{ext}}(\phi) \quad (1)$$

Where $R_p(\phi)$ is the level set regularization term defined in the following, $\mu > 0$ is a constant. The energy $\varepsilon_{\text{ext}}(\phi)$ is the external energy that depends upon the data of an image to be segmented. The energy $\varepsilon_{\text{ext}}(\phi)$ is designed such that it achieves a minimum when the zero level set of the LSF is located at desired position. The level set regularization term $R_p(\phi)$ is defined by

$$R_p(\phi) = \int_{\Omega} p(|\nabla\phi|)d\mathbf{x} \quad (2)$$

Where p is an energy density function, $p:[0,\infty)\rightarrow\Re$.

To avoid the side effect, the energy density function p in the distance regularization term is constructed as follow

$$p(s) = \begin{cases} \frac{1}{(2\pi)^2}(1 - \cos(2\pi s)), & \text{if } s \leq 1 \\ \frac{(s-1)^2}{2}, & \text{if } s \geq 1 \end{cases} \quad (3)$$

This potential $p(s)$ has two minimum points at $s=0$ and $s=1$. Its first and second derivatives given by

$$p'(s) = \begin{cases} \frac{1}{(2\pi)} \sin(2\pi s), & \text{if } s \leq 1 \\ (s-1), & \text{if } s \geq 1 \end{cases} \quad (4)$$

$$p''(s) = \begin{cases} \cos(2\pi s), & \text{if } s \leq 1 \\ 1, & \text{if } s \geq 1 \end{cases} \quad (5)$$

Then, to minimize the energy function $\varepsilon(\phi)$, a standard method is used to find the steady state solution of the gradient flow equation

$$\frac{\partial \phi}{\partial t} = -\frac{\partial \varepsilon}{\partial \phi} \quad (6)$$

Where $\partial \varepsilon / \partial \phi$ is the Gâteaux derivative of the function $\varepsilon(\phi)$. This is an evolution equation of a time-dependent function $\phi(\mathbf{x}, t)$ with a spatial variable x in the domain Ω and a temporal variable $t \geq 0$, and the evolution starts with a given initial function $\phi(\mathbf{x}, 0) = \phi_0(\mathbf{x})$.

The Gâteaux derivative of the function $\mathbf{R}_p(\phi)$ in (2) is

$$\frac{\partial \mathbf{R}_p}{\partial \phi} = -\text{div}(d_p(|\nabla \phi|) \nabla \phi) \quad (7)$$

Where d_p is a function defined by

$$d_p \square \frac{p'(s)}{s} \quad (8)$$

It is easy to verify that the function d_p satisfies

$$|d_p(s)| < 1, \text{ for all } s \in (0, \infty) \quad (9)$$

$$\lim_{s \rightarrow 0} d_p(s) = \lim_{s \rightarrow \infty} d_p(s) = 1 \quad (10)$$

Therefore,

$$|\mu d_p(|\nabla \phi|)| \leq \mu.$$

The gradient flow of the energy $\varepsilon(\phi)$ can be expressed as

$$\frac{\partial \phi}{\partial t} = \mu \text{div}(d_p(|\nabla \phi|) \nabla \phi) - \frac{\partial \varepsilon_{ext}}{\partial \phi} \quad (11)$$

This partial differential equation is the level set evolution equation derived from the proposed variation formulation (1) and is called as a DRLSE for its intrinsic capability of preserving the signed distance property of the LSF, which is associated with the distance regularization term $\mathbf{R}_p(\phi)$ in (1). This partial differential equation can be solved with the Neumann boundary condition and a given initial function ϕ_0 .

3. Segmentation of the Prostate Based on DRLSE

Because of the special location and complex anatomical structures of the prostate, the segmenting of prostate will be divided into two steps. The first step is to segment prostate

from the complex environment adjacent to surrounding tissue, realize the prostate external segmentation. Then, according to the internal anatomy district division of prostate, the prostate internal segmentation is realized. Magnetic resonance imaging of prostate includes T1 and T2 images. Because normal prostate show the similar muscle homogeneous medium signal on the T1WI, it is difficult to distinguish the anatomical relationship of internal district, and the outside around prostate capsule is venous plexus and shows high signal. So T1 image can clearly display the prostate from surrounding environment, and T2 magnetic resonance signal shows a clear internal structure of prostate. When the outer contour of prostate has not yet been separated from surrounding environment, the grey value of internal areas of prostate will interfere in the outside contour segmentation and extraction of prostate. Therefore, this paper will realize the segmentation of outer contour of prostate based on T1 cross sectional shaft images of magnetic resonance.

3.1. Preprocessing

In clinical application, a MR image of a prostate generally contains a complete human body section. The most area in the image are air and the human body structures, such as skin, muscles and bones and the prostate only accounts for a small fraction of the image. If we directly segment the image, there is more redundant information which may bring interference to the segmentation algorithm. So, this paper firstly preprocesses the MR image of the prostate to get a smaller area including the prostate and extract relevant parameters at the same time.

We use prior knowledge to estimate roughly of the prostate's true position, orientation and size obtained based on the profile (the intensity values) along vertical and horizontal direction of the MR image of prostate. We can see the profile image corresponding to the prostate boundary as a roughly rectangular shape. By detecting the left, right, top, and bottom boundary of the prostate in the every slice, we can calculate the center of the prostate as initial estimates of the prostate location.

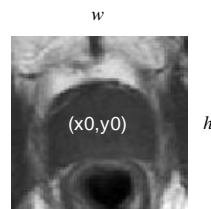


Figure 1. A Prostate MR Image to be Preprocessed

The parameters of MR image include the width, height and center point of the prostate. Let w be the width, h be the height and (x_0, y_0) be the center point. So, the prostate area satisfies

$$\begin{cases} x_0 - c \cdot h < x < x_0 + c \cdot h \\ y_0 - c \cdot w < y < y_0 + c \cdot w \end{cases} \quad (12)$$

Where c is a constant, $0.5 < c < 1$, to control the size of the prostate. As a result of the prostate size is estimated more roughly, we can increase the value of c appropriately to ensure that the area contains the complete prostate. The extracted image including a complete prostate is shown in Figure 1.

3.2. Segmentation of the Prostate

Let I be the prostate image achieved by preprocessing, an edge indicator function g is defined by

$$g \square \frac{1}{1+|\nabla G_\sigma * I|^2} \quad (13)$$

Where G_σ is a Gaussian kernel with a standard deviation σ . The convolution in (13) is used to smooth the prostate image to reduce the noise. This function g usually takes smaller values at prostate boundaries than at other locations.

For a LSF $\phi: \Omega \rightarrow \mathfrak{R}$, we define an energy function $\varepsilon(\phi)$ by

$$\varepsilon(\phi) = \mu R_p(\phi) + \lambda E_{1g}(\phi) + \alpha E_{2g}(\phi) \quad (14)$$

Where $R_p(\phi)$ is the level set regularization term defined in (2), μ is a constant, $\lambda > 0$ and $\alpha \in \mathfrak{R}$ are the coefficients of the energy functions $E_{1g}(\phi)$ and $E_{2g}(\phi)$, which are defined by

$$E_{1g}(\phi) \square \int_{\Omega} g \delta(\phi) |\nabla \phi| dx \quad (15)$$

$$E_{2g}(\phi) \square \int_{\Omega} g H(-\phi) dx \quad (16)$$

Where δ and H are the Dirac delta function and the Heaviside function, respectively.

With the Dirac delta function δ , the energy $E_{1g}(\phi)$ computes the line integral of the function along the zero level contour of ϕ . The energy functional $E_{2g}(\phi)$ computes a weighted area of the region $\Omega_\phi^- \square \{\mathbf{x}: \phi(\mathbf{x}) < 0\}$.

In practice, the Dirac delta function δ and Heaviside function H in the functions $E_{1g}(\phi)$ and $E_{2g}(\phi)$ are approximated by the following smooth functions δ_ε and H_ε as in many level set methods defined by

$$\delta_\varepsilon = \begin{cases} \frac{1}{2\varepsilon} \left[1 - \sin\left(\frac{\pi x}{\varepsilon}\right) \right], & |x| \leq \varepsilon \\ 0, & |x| > \varepsilon \end{cases} \quad (17)$$

and

$$H_\varepsilon = \begin{cases} \frac{1}{2} \left[1 + \frac{x}{\varepsilon} + \frac{1}{\pi} \cos\left(\frac{\pi x}{\varepsilon}\right) \right], & |x| \leq \varepsilon \\ 0, & x > \varepsilon \\ 0, & x < -\varepsilon \end{cases} \quad (18)$$

Note that δ_ε is the derivative of H_ε , i.e., $H'_\varepsilon = \delta_\varepsilon$.

With the Dirac delta function δ and Heaviside function H in (15) and (16) being replaced by δ_ε and H_ε , the energy function $\varepsilon_\varepsilon(\phi)$ is then approximated by

$$\varepsilon_\varepsilon(\phi) = \mu \int_{\Omega} p(|\nabla \phi|) dx + \lambda \int_{\Omega} g \delta_\varepsilon(\phi) |\nabla \phi| dx + \alpha \int_{\Omega} g H_\varepsilon(-\phi) dx \quad (19)$$

This energy function (19) can be minimized by solving the following gradient flow:

$$\frac{\partial \phi}{\partial t} = \mu \operatorname{div} \left(d_p(|\nabla \phi|) \nabla \phi \right) + \lambda \delta_\varepsilon(\phi) \operatorname{div} \left[g \frac{\nabla \phi}{|\nabla \phi|} \right] + \alpha g \delta_\varepsilon(\phi) \quad (20)$$

Given an initial LSF $\phi(x, 0) = \phi_0(x)$. The first term on the right hand side in (20) is associated with the distance regularization energy $R_p(\phi)$, while the second and third terms are associated with the energy terms $E_{1g}(\phi)$ and $E_{2g}(\phi)$, respectively.

The DRLSE in (20) can be implemented with a simple finite difference scheme as follows. The temporal partial derivative $\partial \phi / \partial t$ is approximated by the forward difference. The time dependent LSF $\phi(x, y, t)$ is given in discretized form $\phi_{i,j}^k$ with spatial index (i, j)

and temporal index k . Then, the level set evolution equation is discretized as the following finite difference equation

$$\phi_{i,j}^{k+1} = \phi_{i,j}^k + \Delta t L(\phi_{i,j}^k), \quad k = 0, 1, 2, \dots \quad (21)$$

Where $L(\phi_{i,j}^k)$ is the approximation of the right hand side in the evolution equation. The equation (21) is an iteration process used in the numerical implementation of DRLSE so as to realize the segmentation of prostate.

4. Experiment Results

In DRLSE model (20), there are parameters λ, μ, α and ε , which can be generally fixed for most of applications. But the impact of these parameters on the image segmentation is not analyzed in [16]. So, this section firstly discusses the effects of these parameters on the segmentation of prostate by respectively changing parameter value for one image. Then, we sum up the best range of each parameter and use these results to segment other sample images. The magnetic resonance images of prostate used in this section is offered by Harbin Humor Hospital and come to 30 images from 10 cases including normal cases, benign hyperplasia cases and cancer cases.

The effect on segmentation of parameter λ is shown in Table 1. The best value range of parameter λ is between 1 and 3. When parameter λ is less than 1, the iteration times increase obviously. However, when parameter λ is greater than 3, it is difficult to get an optimal result by increasing the iteration times.

Table 1. Effect on Segmentation of the Parameter λ

λ	$\lambda < 1$	$1 \leq \lambda \leq 3$	$\lambda > 3$
Result	The iteration times increase obviously.	After 360 iterations, the result is close to an optimal result.	Although we increase the iteration times, it is difficult to get an optimal result.

The effect on segmentation of parameter α is shown in Table 2. It can be easily seen from Table 2 that when the absolute value of α becomes greater, the iterations decrease. But when the absolute value of α is greater than 5, the iterations basically remain unchanged. It is not difficult to conclude that the parameter α has not obvious impact on the segmentation of the prostate. Generally, we can select a value between -2 and -8 for MRI segmentation of the prostate.

Table 2. Effect on Segmentation of the Parameter α

α	$\alpha = -2$	$\alpha = -3$	$\alpha = -4$	$\alpha = -5$	$\alpha = -6$	$\alpha = -8$
Iterations	510	360	260	210	210	210

The effect on segmentation of parameter ε is shown in Table 3. The best value range of parameter ε is between 1 and 2. When parameter ε is less than 1, the iteration times increase obviously, but it is difficult to get an optimal result. When parameter ε is greater than 2, the iterations are decreased, but the image leaks.

Table 3. Effect on Segmentation of the Parameter ε

ε	$\varepsilon < 1$	$1 \leq \varepsilon \leq 2$	$\varepsilon > 2$
Result	Although we increase the iteration times, it is difficult to get an optimal	After 310 iterations, the result is close to an	Although the iteration times are decreased, the image leaks, as shown in

	result, as shown in Figure 4(a).	optimal result.	Figure4 (c).
--	----------------------------------	-----------------	--------------

The effect on segmentation of parameter μ is shown in Table 4. It can be easily seen from Table 4 that when the value of μ becomes greater, the iterations increase. The parameter μ has not important impact on the segmentation of the prostate. Generally, we can select 0.2 as the value of μ for MRI segmentation of the prostate.

Table 4 Effect on Segmentation of the Parameter μ

μ	$\mu=0.04$	$\mu=0.1$	$\mu=0.2$	$\mu=0.4$
Iterations	110	160	260	360

As discussed above, different parameter has different impact on MRI segmentation of the prostate. To verify the MRI segmentation method of a prostate present in this paper, we select $\lambda=2$, $\alpha=-6$, $\varepsilon=1.5$ and $\mu=0.2$ to segment a part of images from normal prostate, benign hyperplasia prostate and cancer prostate. Figure 2 shows the MRI segmentation results of three continuous slices of one normal prostate. The MRI segmentation results of three continuous slices of one benign hyperplasia prostate are shown in Figure 3 Figure 4 shows the MRI segmentation results of three continuous slices of one cancer prostate. From these figures, it can be seen easily that the segmentation results (white lines) using the algorithm present in this paper are similar to the segmentation results (black lines) using hands. So we can conclude that the MRI segmentation method of prostate presented is effective for different situation of different patients.

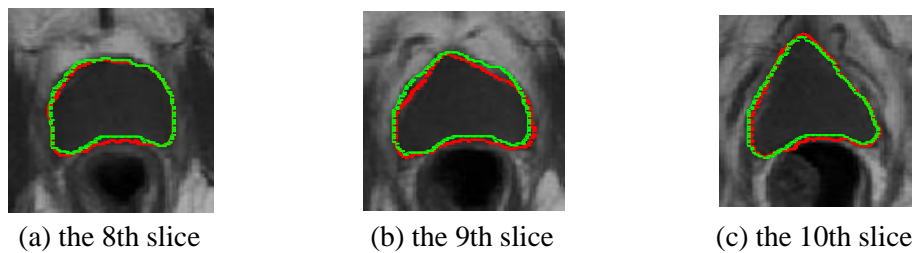


Figure 2. MRI Segmentation Results of a Normal Prostate

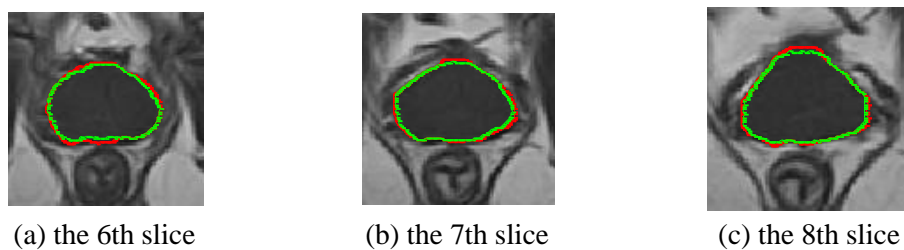


Figure 3. MRI Segmentation Results of a Benign Hyperplasia Prostate

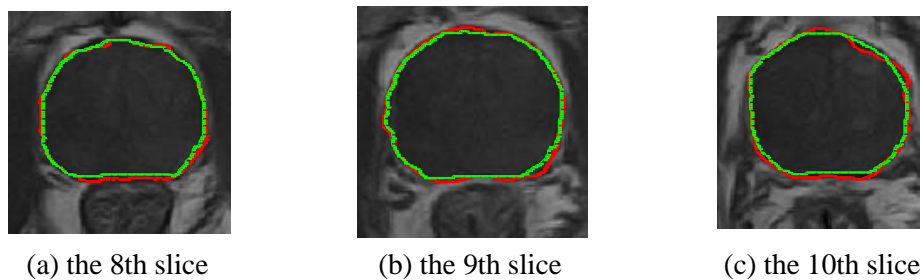


Figure 4. MRI Segmentation Results of a Cancer Prostate

5. Conclusion

A MR T1 image segmentation method of a prostate based on DRLSE is presented in this paper. There are parameters λ , μ , α and ε in DRLSE model and the effects of these parameters on the segmentation of a prostate are discussed. As the results of experiments, the best value range of parameter λ is 1 to 3; meanwhile the best value range of parameter ε is 1 to 2. To shorten the segmentation time, we may select a relatively smaller value of parameter μ and α for most applications, generally $\mu=0.2$ and $\alpha=-6$. To verify the effectiveness of the MR T1 image segmentation method of a prostate, we segment a part of images from normal prostate, benign hyperplasia prostate and cancer prostate. The results show that the method is effective for different situation of different patients.

Acknowledgements

This research was supported by the National Natural Science Foundation of China (Grant No 51305107), Research Fund for the Doctoral Program of Higher Education of China (Grant No. 20122303110006), Natural Science Foundation of Heilongjiang Province of China (Grant Nos E2015059, E201448).

Reference

- [1] J. C. Weinreb and F. V. Coakley, "MR Imaging and MR Spectroscopic Imaging of Prostate Cancer Prior to Radical Prostatectomy: a Prospective Multi-Institutional Clinic Opathological Study", Presented at RSNA, Chicago, IL, (2006).
- [2] G. Litjens, R. Toth and W. Van De Ven, "Evaluation of prostate segmentation algorithms for MRI: the promise12 challenge", *Medical Image Analysis*, no. 18, (2014), pp. 359–373.
- [3] D. Pasquier, T. Lacomberie, M. Vermandel, J. Rousseau, E. Lartigau and N. Betrouni, "Automatic segmentation of pelvic structures from magnetic resonance images for prostate cancer radiotherapy", *Int. J. Radiat. Oncol. Biol. Phys.*, no. 68, (2007), pp. 592–600.
- [4] R. Toth, B.N. Bloch, E.M. Genega, N.M. Rofsky, R.E. Lenkinski, M.A. Rosen, A. Kalyanpur, S. Pungavkar and A. Madabhushi, "Accurate prostate volume estimation using multifeature active shape models on T2-weighted MRI", *Acad. Radiol.*, vol. 18, (2011), pp. 745–754.
- [5] Y. Hu, H.U. Ahmed, Z. Taylor, C. Allen, M. Emberton, D. Hawkes and D. Barratt, "MR to ultrasound registration for image-guided prostate interventions", *Med. Image Anal.*, no. 16, (2012), pp. 687–703.
- [6] P.C. Vos, J.O. Barentsz, N. Karssemeijer and H.J. Huisman, "Automatic computer aided detection of prostate cancer based on multiparametric magnetic resonance image analysis", *Phys. Med. Biol.*, no. 57, (2012), pp. 1527–1542.
- [7] P. Tiwari, J. Kurhanewicz and A. Madabhushi, "Multi-kernel graph embedding for detection, gleason grading of prostate cancer via MRI/mrs", *Med. Image Anal.*, no. 17, (2013), pp. 219–235.
- [8] S. Chandra, "Patient specific prostate segmentation in 3-D magnetic resonance images", *IEEE Trans. Med. Imag.*, (2012), pp. 1955–1964.
- [9] S. Ghose, "Graph cut energy minimization in a probabilistic learning framework for 3D prostate segmentation in MRI", 21st International Conference on Pattern Recognition, (2012), pp. 125–128.

- [10] S. Chandra, J. Dowling and K. Shen, “Automatic segmentation of the prostate in 3D magnetic resonance images using case specific deformable models”, International Conference on Digital Image Computing: Techniques and Applications, (2011), pp. 7-12.
- [11] Y. Artan, “Prostate cancer segmentation using multispectral random walks”, MICCAI'10 proceedings of the 2010 international conference on prostate cancer Imaging: computer-aided diagnosis, prognosis, and intervention, (2010), pp. 15-24.
- [12] M. Yang and X. Li, “Prostate segmentation in MR images using discriminant boundary features”, IEEE Transactions on Biomedical Engineering, vol. 60, no. 2, (2013), pp. 479.
- [13] Xin Liu, Masoom A. Haider and Imam Samil Yetik, “Unsupervised 3D prostate segmentation based on diffusion-weighted imaging MRI using active contour models with a shape prior”, Hindawi Publishing Corporation Journal of Electrical and Computer Engineering, (2011), pp. 1-11.
- [14] W. Xiong, “Automatic 3D prostate MR image segmentation using graph cuts and level sets with shape prior”, Advances in Multimedia Information Processing – PCM 2013, Lecture Notes in Computer Science, (2013), pp. 211-220.
- [15] R. Toth and A. Madabhushi, “Multi-feature landmark-free active appearance models: application to prostate MRI segmentation”, IEEE Trans. Med. Imag., (2012), pp.1638–1650.
- [16] C. Li, C. Xu, C. Gui and M. D. Fox, “Distance regularized level set evolution and its application to image segmentation”, IEEE Transactions on Image Processing, vol. 12, no. 19, (2010), pp. 3243-3254.

